Key Engineering Materials
ISSN: 1662-9795, Vol. 1047, pp 373-382

Submitted: 2026-01-23
Accepted: 2026-02-11
Online: 2026-04-13

Additive Manufacturing of Automotive Metal Multi-Material Shunt Resistor: Cost and Carbon Footprint Analysis

Nikolaos D. Alexopoulos[1,a*], Vasileios Zeimpekis[1,b], Evangelos Vasileiou[1,c], Theodoros Souxes[1,d], Ilona Lazaridou[1,e], Leonard Alberty[2,f], Ismail Ünsal[2,g], Georg Schlick[2,h]

[1]University of the Aegean, School of Engineering, Department of Financial and Management Engineering, Research Unit of Advanced Materials, 41 Kountouriotou str, 82132, Chios, Greece

[2]Fraunhofer Institute for Casting, Composite and Processing Technology IGCV, Am Technologiezentrum 10, 86159 Augsburg, Germany

[a*]nalexop@aegean.gr, [b]vzeimp@aegean.gr, [c]evasileiou@hmu.gr, [d]theosouxes@gmail.com, [e]lazaridou.ilona@gmail.com, [f]leonard.alberty@igcv.fraunhofer.de, [g]ismail.uensal@igcv.fraunhofer.de, [h]georg.schlick@igcv.fraunhofer.de

Keywords: additive manufacturing, metallic multi-material 3D printing, ABC costing, carbon footprint, automotive shunt resistor, manganin-copper alloys.

Abstract. Additive manufacturing (AM) transforms automotive production by enabling lightweight, complex components with reduced material waste. The present contribution investigates multi-material AM for automotive demonstrators combining copper-manganese-nickel and copper alloys, leveraging their complementary structural, thermal, and electrical properties. Such a component from the automotive sector is benchmarked against the respective conventionally manufactured part. Key performance indicators include structural weight, manufacturing cost via Activity-Based Costing, production time, energy consumption, and CO_2 emissions. Although this investigation compares AM laboratory/semi-industrial-scale and conventional industrial-scale implementations, the multi-material AM can deliver significant system-level benefits in energy efficiency and vehicle performance. These advantages are realized despite existing challenges related to interfacial bonding and process integration, and notwithstanding the associated increases in weight, cost and carbon footprint.

Introduction

The automotive industry faces increasing pressure from sustainability regulations, electrification, and demand for lightweight, high-performance vehicles. Traditional manufacturing methods, such as casting, forging, and machining, are limited in design flexibility and the integration of dissimilar metals [1], [2]. Additive manufacturing (AM) produces parts layer-by-layer, enabling complex geometries and multi-material integration [3], [4].

Copper-manganese-nickel (here after called Manganin) material is widely used for precision electrical applications -especially shunt resistors- because of its low temperature coefficient of resistance, stable resistivity, and excellent long-term electrical stability [5], while copper alloys provide excellent electrical and thermal conductivity, essential for electric vehicle components [6], [7]. Conventional approaches combine these materials through assembly, adding weight and complexity. Multi-material AM enables single components with spatially distributed Manganin and copper alloys, optimizing structural, thermal, and electrical performance. Techniques such as directed energy deposition (DED), laser powder bed fusion (PBF-LB/M), and friction stir additive manufacturing allow graded properties and strong interfacial bonding, e.g. [8], [9], [10].

Challenges include thermal expansion mismatch, intermetallic formation, and achieving defect-free bonds. Economic and environmental comparisons with conventional methods remain limited [11], nevertheless this kind of assessment is crucial for industrial adoption. The present investigation evaluates Manganin-Copper demonstrators through process mapping, cost analysis, and life cycle assessment, highlighting the technical, economic, and environmental trade-offs of multi-material AM in automotive applications.

Cost and Environmental Analysis

Activity-Based Costing (ABC) for Additive Manufacturing.

To evaluate the economic feasibility of multi-material additive manufacturing (AM) for Manganin-copper automotive components, the Activity-Based Costing (ABC) methodology was applied [12]. ABC assigns both direct and indirect costs to specific activities, providing a granular understanding of cost drivers across the production process [13]. The ABC approach involves:

1. Identifying the resources consumed in part production (e.g., materials, machine usage, labour).
2. Assigning resource costs to relevant activities based on consumption.
3. Breaking down the manufacturing process into activities such as part preparation, machine operation, post-processing, and quality control.
4. Allocating costs to each activity using appropriate cost drivers (e.g., machine hours, setup time).
5. Aggregating activity costs to obtain the total part cost.

ABC is particularly suitable for multi-material AM in the automotive sector because these processes often involve complex interactions between materials, multiple process steps, and high indirect costs (e.g., interfacial bonding, graded material deposition, and post-processing). Unlike traditional costing methods, ABC captures the cost impact of these process-specific activities, enabling accurate benchmarking against conventional manufacturing routes. Moreover, ABC provides insights into economies of scale and resource optimization, which are critical for industrial adoption of multi-material components in high-performance vehicle applications.

Carbon Footprint Assessment via Life Cycle Assessment (LCA).

The environmental impact of multi-material AM components was quantified using Life Cycle Assessment (LCA), focusing on equivalent carbon emissions (carbon footprint). LCA evaluates the greenhouse gas emissions associated with a product throughout its life cycle, from raw material extraction to manufacturing. For this study, the assessment followed ISO standards and the PAS2050 methodology [14], covering the manufacturing phase. The procedure included:

1. mapping the production process and defining system boundaries,
2. collecting data on material use, energy consumption, and process emissions, and
3. calculating the carbon footprint using *LCA for Experts* software (formerly GaBi) provided by Sphera©, which integrates global warming potential data for metals and industrial manufacturing processes, such as copper-manganese alloys.

LCA is particularly appropriate for multi-material automotive AM since these processes can involve energy-intensive steps (e.g., laser-based powder bed fusion, directed energy deposition) since the process parameters are different for the different materials and build jobs (due to the different metals involved). Evaluating the environmental impact at the activity level allows identification of hotspots, such as material melting or post-processing, and supports comparison with conventional manufacturing techniques. This makes LCA a robust tool for quantifying system-level sustainability benefits, including potential reductions in energy use, material waste, and CO_2 emissions in the production of lightweight automotive components.

Description of the Shunt Resistor Demonstrators and the Manufacturing Processes

Conventional and Additive Manufacturing Fabrication.

The examined automotive demonstrator is provided within the Horizon Europe project "MADE-3D" by the industrial partners AVL and Fraunhofer Institute for Casting, Composite and Processing Technology IGCV for the conventional and AM production respectively. It consists of a multi-material current measurement sensor (Shunt Resistor). Shunt resistors enable the measurement of high currents that cannot be determined directly. In this demonstrator, the current flows through the resistive section of the shunt, which is subsequently integrated with conventional machining post-processing. The resulting voltage drop across the resistive section is proportional to the current, allowing direct measurement through scaling. The resistance is selected to minimize both measurement error and waste heat generation.

The materials used for the shunt resistor are Cu-ETP (Electrolytic Tough Pitch with ≥ 99.90 % Cu, ≤ 0.04 % O, ≤ 0.005 % Pb, ≤ 0.0005 % Bi, and < 0.03 % total other impurities) and Manganin (84 % copper, 12 % manganese and 4 % nickel). Conventional shunts are typically simple, one-directional conductors with known resistance, but they cannot operate continuously at high currents for extended periods due to thermal limitations. The resistive section generates heat during operation, leading to resistance changes: for Manganin, thermal drift begins at 80 °C, becomes significant at 120 °C, and permanent damage occurs at 140 °C. Moreover, high-current operation produces unwanted electromagnetic fields, which can adversely affect nearby electronic systems. Multi-material additive manufacturing allows the integration of Cu-ETP and Manganin in a single component, optimizing electrical, thermal, and structural performance while potentially reducing assembly complexity, material waste, and overall environmental impact.

In Fig. 1(a), the conventionally manufactured shunt resistor BAX-Z-L005-01-5.0 by Isabellenhuette USA is shown, whereas Fig. 1(b) presents the 3D-printed multi-material demonstrator fabricated by IGCV, along with four rectangular witness specimens.

(a) (b)

Fig. 1. Schematic representation of the fabricated Shunt Resistor; (a) conventional, and (b) IGCV 3D-printed.

Manufacturing Processes.

As far as the manufacturing processes of the examined use-cases are concerned, the manufacturing stages of the analysed demonstrators are categorized into three subprocesses, as outlined below, to facilitate a more detailed examination of each process. This approach enables the identification of cost-generating activities and the calculation of energy consumption, material usage, labour, total manufacturing costs, and carbon footprint. To this end, the whole manufacturing process and activities for the construction of the metal multi-material conventional and AM components was identified and categorized into the following three (3) main sub-processes:

a) Sub-process 1: preparation of the materials, environment and computer systems,
b) Sub-process 2: main process/conventional or 3D-printing fabrication of the component, and
c) Sub-process 3: post process including quality evaluation, inspection and cleaning.

As far as conventional manufacturing is concerned, the preparation stage includes all activities carried out before the main processing of the AVL shunt resistor, focusing on readying the Cu-ETP and Manganin materials for welding and stamping. The raw materials are first pre-processed, after

which the two copper side bars and the Manganin strip are loaded and fixed in a jig, and the welding area is machined. The preparation phase concludes with washing the part in a conveyor-type cleaning machine. The main processing stage covers the welding, stamping and formation of the final product: the three components are welded along their full-length using electron-beam welding, the individual shunts are stamped out, and a second washing cycle is performed in batch mode. In the post-processing stage, product quality is evaluated by sampling 1 % of the lot for 3D dimensional measurement, while all parts undergo end-of-line resistance testing, marking, and visual inspection to detect flaws. The process concludes with the final packing of the components.

For the additive manufacturing route, the preparation stage encompasses all activities required before printing, including the preparation of the digital build data, the conditioning and inspection of the powder materials, and the setup and calibration of the machine. The main processing stage consists of five successive build jobs—Cu–Manganin–Cu–Manganin–Cu—each printed with a small layer thickness and separated by full machine cleaning cycles, with four rectangular witness specimens fabricated alongside the demonstrator. Finally, post-processing activities include removing the printed part from the build plate, de-powdering and cleaning the component, and cutting operations to separate or finish functional sections, completing the AM manufacturing workflow.

Cost estimation Relationships (CERs) and Analysis

In this section, the methodology used for the economic evaluation of the AVL-IGCV components manufacturing processes is presented. The total manufacturing cost per sub-process consists of energy consumption, material, labour cost, as well as depreciation of used fixed asset.

Energy consumption (EC).

The relationship used for the energy consumption cost is as follows:

$$EC_x = Set\ Up\ Cost + Operationg\ Cost = \left(IC_x \cdot PC_x \cdot T_{SU_x} \cdot CE\right) + (IC_x \cdot PC_x \cdot T_x \cdot CE), \quad (1)$$

where $\boldsymbol{IC_x}$ is the rated power (installed capacity) of the machine, $\boldsymbol{PC_x}$ denotes the power utilization (capacity range) percentage of the machine during the specific sub-process, $\boldsymbol{T_{SU_x}}$ signifies the per unit initial processing operating time of the machine (measured in hours), $\boldsymbol{T_x}$ represents the per unit operating time during the specific sub-process (in hours), *x* denotes the activity examined and $\boldsymbol{CE}$ is the cost of electricity (in € /kWh).

Material Cost (MC).

The material cost pet unit is equal to:

$$MC_x = \sum_{i=1}^{k}\{W_x \cdot P_{M_i}\}, \quad (2)$$

where $\boldsymbol{W_x}$ is the weight of the material waste lost due to agglomeration and loss of shape (in kg), *x* denotes the activity examined and $\boldsymbol{P_{M_i}}$ is the purchase price of the material $\boldsymbol{i}$ (in €/kg).

Labor Cost (LC).

The formula for the labour cost entails the aggregation of the labour cost attributed to the set-up technician, alongside the labour cost associated with skilled and unskilled workers (with consideration given to the inclusion of all skilled-level workers within a given sub-process):

$$LC_x = Set\ Up\ Cost + Operationg\ Cost = \left(T_{SU_x} \cdot CH_{SUT}\right) + \left[\left(T_{UW_x} \cdot CH_{UW} + T_{SW_x} \cdot CH_{SW}\right)\right], \quad (3)$$

where $\boldsymbol{T_{SU_x}}$, $\boldsymbol{T_{UW_x}}$ and $\boldsymbol{T_{SW_x}}$ are the set-up technician's/ unskilled / skilled worker's operating times (in hours) respectively, $\boldsymbol{x}$ denotes the activity examined and $\boldsymbol{CH_{SUT}}$, $\boldsymbol{CH_{UW}}$ and $\boldsymbol{CH_{SW}}$ represent the labour cost per hour required for the production of one unit (measured in €/h), contingent upon the level of skills involved (Set-Up Technician, Unskilled and Skilled Worker).

Rental Cost (RC).

The rental cost of the examined activity *x* is calculated based on the relationship:

$$RC_x = SQM_x \cdot R_{sqm} \cdot \frac{12}{APR}, \quad (4)$$

where SQM_x are the square meters used in the activity *x,* R_{sqm} is the rent cost per month for each square meter, multiplied by 12 in order to estimate the yearly cost and divided by the APR annual production rate (in units), in order to have an estimation for the cost per unit.

Depreciation Cost (DC).

The depreciation charge of fixed equipment is calculated as follows:

$$DC_x = \frac{DC_{EQUIP_x}}{DP_x \cdot APR}, \quad (5)$$

where DC_{EQUIP_x} is the investment-depreciation cost of the machine-equipment (in € / year) used in the activity x, DP_x is the depreciation period (in years) of the equipment and APR is the annual production rate (in units), in order to have an estimation for the cost per unit.

Machine Variable Cost (MVC).

The per unit machine variable cost is calculated as:

$$MVC_x = \frac{MV_{EQUIP_x}}{APR}, \quad (6)$$

where MV_{EQUIP_x} is the variable cost of the machine-equipment (in € / year) used in the activity x and APR is the annual production rate (in units).

Total Manufacturing Cost (TC).

The total manufacturing cost (TC) of the activity x is the sum of all previous costs, Eq. 1-6, given as follows:

$$TC_x = (EC_x + MC_x + LC_x + RC_x + MVC_x + DC_x). \quad (7)$$

It should be noted at this point that the cost model additionally incorporates material overheads (e.g., consumables; material procurement; incoming-goods handling, inspection, and storage/inventory management) and manufacturing overheads (e.g., indirect personnel; general equipment; auxiliary operating supplies; ancillary materials). Nevertheless, a more detailed disaggregation of these overhead categories is not presented herein for reasons of scope and focus.

Conventional and Additive Manufacturing Demonstrators Comparison

Weight comparison results.

By directly comparing the two shunt resistors (conventional and 3D-printed) in terms of structural weight, Table 1 shows that there is a weight increase in the innovative AM multi-material technology case.

Table 1. Structural weight comparison of the fabricated shunt resistors.

	Conventional [g]	Additive Manufactured [g]
Manganin	5	13
Cu-ETP	100	120
Total	105	139

Cost analysis results.

A cost comparison between the conventional and AM demonstrators is performed for both the individual cost categories and the corresponding sub-processes, based on the equations and methodology presented in the previous section (Eqs. 1–7). The sub-process cost breakdown for the shunt resistor components is summarized in Table 2 and illustrated in Fig. 2, while a comparison of the aggregated individual cost categories is provided in Table 3.

Table 2. Comparison of the individual sub-processes' costs of the conventional and 3D-printed shunt resistor components (*CAI = Cost Amount Indicator).

	Conventional		Additive Manufacturing	
	CAI* (-)	Weight (%)	CAI* (-)	Weight (%)
SP1	2.25	32.20 %	5.90	16.10 %
SP2	1.95	27.92 %	24.97	68.09 %
SP3	0.92	13.12 %	1.71	4.65 %
Overheads	1.87	26.77 %	4.09	11.16 %
Total	6.98	100.00 %	36.67	100.00 %

Table 3. Comparison of individual category costs of the conventional and IGCV 3D-printed demonstrator (*CAI = Cost Amount Indicator).

Category	Conventional CAI* [-]	Additive Manufacturing CAI* [-]
D (depreciation)	0.97	14.85
E (energy)	0.37	2.34
L (labour)	1.78	7.01
M (materials)	1.58	2.38
MV (machine variable)	0.38	4.67
O (overheads)	1.87	4.09
R (rental)	0.04	1.33
Total	6.98	36.67

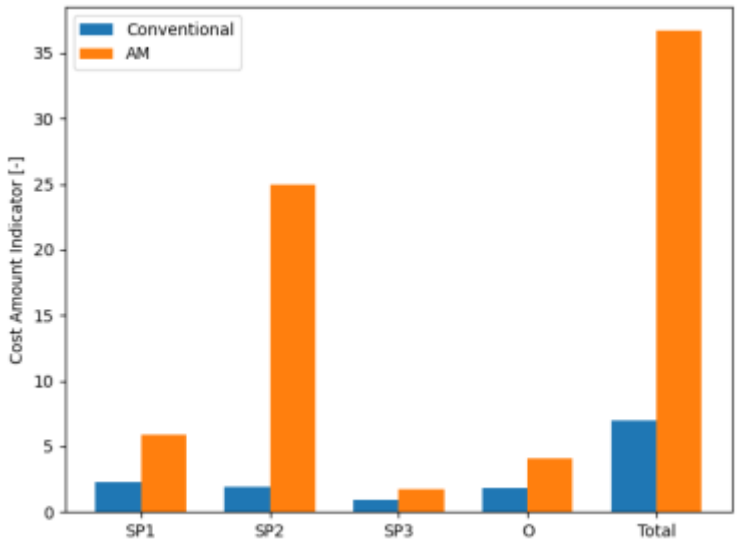

Fig. 2. Schematic Comparison of the individual sub-processes' costs of the conventional and 3D-printed shunt resistor demonstrators (*CAI = Cost Amount Indicator).

As observed in Tables 2 and 3, and clearly illustrated in Fig. 2, the main sub-process (SP2) exhibits a significantly higher contribution in the AM case. This behaviour is primarily attributed to the substantially longer cycle times of the 3D-printing process at laboratory (or semi-industrial) scale. Consequently, both labour and energy costs are considerably increased for the AM demonstrator.

Moreover, in the conventional manufacturing case, the same production equipment is utilized at industrial scale for multiple products, and therefore depreciation, machine-related variable costs, and rental costs are distributed across a broader production volume. In contrast, for the laboratory-scale 3D-printed shunt resistor, these costs are allocated exclusively to a single demonstrator. This allocation significantly amplifies the corresponding cost categories, leading to a pronounced increase in the overall AM cost. It is highly expected that with the development of multi-functional, higher-dimension machines, increased automation etc. the manufacturing cost will be probably greatly reduced. Additionally, due to their higher efficiency, it is expected that the production time will be greatly decreased by the cooldown time between layers (currently 2-minute minimum time per layer) essentially affecting labour cost.

Carbon footprint assessment results.

Preliminary results of a gate-to-gate approach show that the 3D-printing process produces higher equivalent carbon emissions when compared to the conventional manufacturing process. The latter results since the majority (99 %) of equivalent carbon emissions come from the key process of additive manufacturing, Figure 3. More specifically, the production duration of build job is increased due to the cooldown time between layers resulting to the increase of energy consumption.

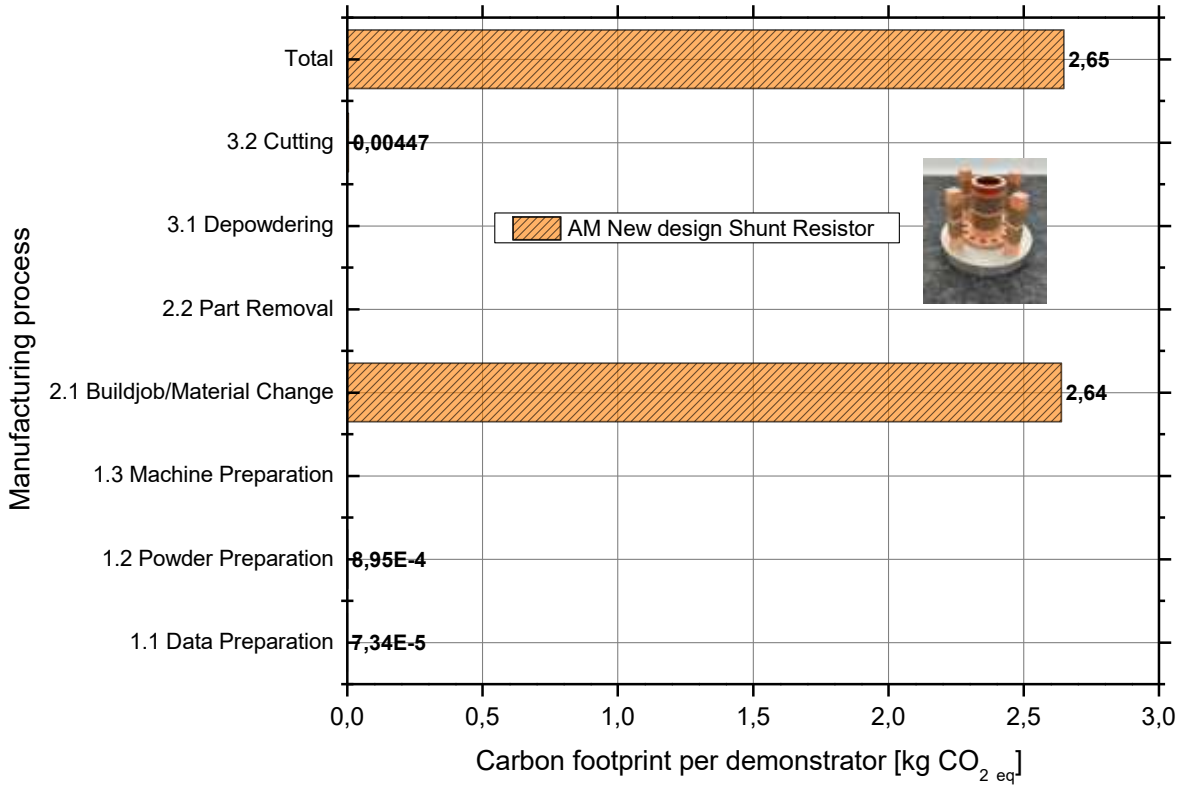

Fig. 3. Carbon footprint (gate to gate) for key manufacturing activities (single demonstrator).

As shown in Figure 4, Sub-Process 2 (SP2) produces the highest carbon footprint emissions for both, conventional as well as the additive manufactured demonstrator. This is since the main production processes are included in SP2. More specifically, the conventional manufacturing SP2 accounts for approximately 44 % of the total equivalent carbon emissions whereas the Additive manufacturing SP2 is responsible for over 99 % of the total emissions. The results reveal that Additive manufacturing is more energy-intensive resulting in almost four times (x4) higher equivalent carbon dioxide emissions.

Overall, from environmental point of view, the additive manufacturing demonstrator appears mostly energy intensive when compared to the conventional manufactured demonstrator. Yet, it is worth investigating and comparing the equivalent carbon emissions that results from the total life cycle of the end-product (cradle to grave), i.e. from raw materials until recycling.

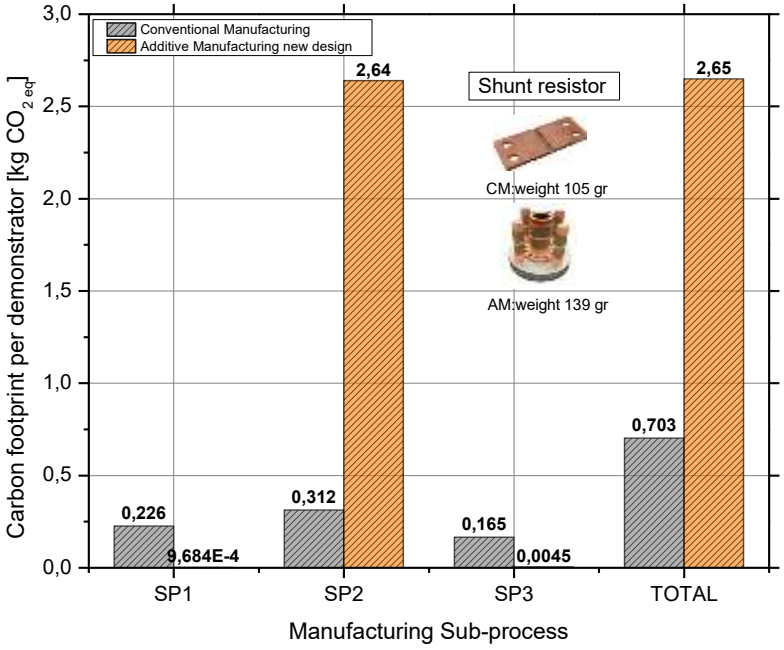

Fig. 4. Comparison of Conventional Manufacturing versus Additive Manufacturing carbon footprint (gate to gate) per Sub process.

Summary

This article investigated the application of multi-material additive manufacturing (AM) for an automotive shunt resistor demonstrator combining Manganin and Cu-ETP alloys, with a systematic comparison against a conventionally manufactured counterpart. The analysis focused on key performance indicators including weight, manufacturing cost, energy consumption, production time, and carbon footprint, using Activity-Based Costing (ABC) and Life Cycle Assessment (LCA) methodologies.

The results indicate that the AM demonstrator exhibits a higher total weight compared to the conventional shunt resistor, primarily due to the current design constraints and process requirements at laboratory scale. From an economic perspective, the total manufacturing cost of the AM component is substantially higher. This increase is mainly driven by the main manufacturing sub-process (SP2), where extended cycle times inherent to laboratory-scale multi-material 3D printing led to significantly increased labour and energy costs. In addition, depreciation, machine-related variable costs, and rental costs are disproportionately allocated to a single AM demonstrator, in contrast to conventional industrial-scale production where such costs are distributed across high production volumes.

Similarly, the carbon footprint of the AM demonstrator is higher, reflecting the energy-intensive nature of metal additive manufacturing processes and the limited economies of scale at laboratory implementation. These findings highlight that direct comparisons between laboratory-scale AM, and industrial-scale conventional manufacturing inevitably disadvantage AM in terms of cost and CO_2 emissions.

Despite these results, the study demonstrates that multi-material AM offers important system-level advantages that are not fully captured by unit cost and footprint metrics alone. The integration of Manganin and copper within a single component enables enhanced electrical, thermal, and functional performance, reduced assembly complexity, and new design freedoms that are unattainable with conventional manufacturing routes. These benefits are particularly relevant for advanced automotive

and electrification applications, where performance optimization, functional integration, and lightweight design play a critical role.

Future work will focus on scaling the AM process to an industrial production environment and performing a like-for-like comparison with conventional manufacturing at equivalent production volumes. Further optimization of process parameters, build strategies, and material interfaces is also expected to reduce cycle times, energy consumption, and overall environmental impact. Under such conditions, multi-material AM has the potential to become a competitive and sustainable manufacturing solution for next-generation automotive components.

Acknowledgement

The authors gratefully acknowledge the financial support of the HORIZON Research and Innovation Actions, European Health and Digital Executive Agency for the implementation of the project «MULTI-MATERIAL DESIGN USING 3D PRINTING» having an acronym "MADE-3D" of the act HORIZON-CL4-2022-RESILIENCE-01 with Grant Agreement code 101091911.

References

[1] S. Caba, "Aluminum Alloy for Additive Manufacturing in Automotive Production," *ATZ Worldw.*, vol. 122, no. 11, pp. 58–61, 2020, doi: 10.1007/s38311-020-0285-y.

[2] X. Yu, J. Griffis, G. Manogharan, and A. Panesar, "Multi-material additive manufacturing: a computational design perspective," *Virtual Phys Prototyp*, vol. 20, no. 1, p. e2546671, 2025, doi: 10.1080/17452759.2025.2546671.

[3] S. N. Samad, J. Griffis, G. Manogharan, and N. Kouraytem, "Multi-material additive manufacturing of metals: A review of structures and mechanical characteristics," *Engineering Science in Additive Manufacturing*, vol. 1, no. 2, p. 25180010, 2025, doi: https://doi.org/10.36922/ESAM025180010.

[4] S. M. A. Nipu *et al.*, "Advances and perspectives in multi-material additive manufacturing of heterogenous metal-polymer components," *npj Advanced Manufacturing*, vol. 2, no. 1, p. 31, 2025, doi: 10.1038/s44334-025-00045-w.

[5] S. N. Misti, M. Birkett, R. Penlington, and D. Bell, "Effect of Abrasive Machining on the Electrical Properties Cu86Mn12Ni2 Alloy Shunts," *Materials*, vol. 10, no. 8, 2017, doi: 10.3390/ma10080876.

[6] A. Vahedi Nemani, M. Ghaffari, K. Sabet Bokati, N. Valizade, E. Afshari, and A. Nasiri, "Advancements in Additive Manufacturing for Copper-Based Alloys and Composites: A Comprehensive Review," *Journal of Manufacturing and Materials Processing*, vol. 8, no. 2, 2024, doi: 10.3390/jmmp8020054.

[7] K. Morshed-Behbahani, A. Aliyu, D. P. Bishop, and A. Nasiri, "Additive manufacturing of copper-based alloys for high-temperature aerospace applications: A review," *Mater Today Commun*, vol. 38, p. 108395, Mar. 2024, doi: 10.1016/J.MTCOMM.2024.108395.

[8] I. Wolff, "AM Applications Explode with Multimaterial Printing," *SME*, Jun. 2023, [Online]. Available: https://www.sme.org/technologies/articles/2023/june/am-applications-explode-with-multimaterial-printing/.

[9] D. Gu, X. Shi, R. Poprawe, D. L. Bourell, R. Setchi, and J. Zhu, "Material-structure-performance integrated laser-metal additive manufacturing," *Science (1979)*, vol. 372, no. 6545, p. eabg1487, 2021, doi: 10.1126/science.abg1487.

[10] H. Chen *et al.*, "Wire-based friction stir additive manufacturing of AlCu alloy with forging mechanical properties," *J Manuf Process*, vol. 133, pp. 354–366, Jan. 2025, doi: 10.1016/J.JMAPRO.2024.11.037.

[11] N. Arefin, H.-E.-J. Moni, D. Espinosa, W. Cong, and M. Zeng, “Multi-material additive manufacturing of energy storage and conversion devices: Recent progress and future prospects,” *Appl Phys Rev*, vol. 12, no. 1, p. 011330, Mar. 2025, doi: 10.1063/5.0235864.

[12] R. Cooper and Kaplan Robert S., “Profit Priorities from Activity-Based Costing,” *Harv Bus Rev*, vol. 3, no. 69, pp. 130–135, 1991.

[13] M. Gupta and K. Galloway, “Activity-based costing/management and its implications for operations management,” *Technovation*, vol. 23, no. 2, pp. 131–138, Feb. 2003, doi: 10.1016/S0166-4972(01)00093-1.

[14] B. S. Institution, *Guide to PAS 2050: How to assess the carbon footprint of goods and services*. London: British Standardization Institute, 2008.